



# miR-182-5p Attenuates High-Fat -Diet-Induced Nonalcoholic Steatohepatitis in Mice

Qionghe Liang,<sup>\*,\*\*</sup> Huan Chen,<sup>\*</sup> Xiaoqun Xu,<sup>\*</sup> Weiwei Jiang<sup>\*,\*\*\*</sup>

<sup>\*</sup> Department of Neonatal Surgery, Children's Hospital of Nanjing Medical University, Nanjing, China.

<sup>\*\*</sup> Department of Radiology, Children's Hospital of Nanjing Medical University, Nanjing, China.

<sup>\*\*\*</sup> Institute of Pediatric Research, Children's Hospital of Nanjing Medical University, Nanjing, China.

## ABSTRACT

**Introduction and aim.** Patients with NASH have increased risk for sepsis or cardiovascular disease after Liver transplantation. An important role of Toll-like receptor (TLR) 4 in the pathogenesis of nonalcoholic steatohepatitis (NASH) was demonstrated. Here, we study the role of miR-182-5p in TLR4 expression and high-fat-diet (HFD)-induced NASH *in vitro* and *in vivo*. **Material and methods.** Following transfection with a miR-182-5p mimic, the effect of miR-182-5p on TLR4 in RAW264.7 and HepG2 cells was investigated. Following administration of the miR-182-5p mimic into the livers of HFD-induced NASH mice, we determined the *in vivo* expression of TLR4, TNF $\alpha$ , and IL-6 and assessed the histologic features of the livers. **Results.** Following lipopolysaccharide (LPS) treatment of RAW264.7 cells, real-time RT-PCR and western blot results indicated decreases levels of TLR4 mRNA and protein in the miR-182-5p group as compared with levels observed in controls, with similar trends were observed in TNF $\alpha$  and IL-6 protein levels. Following oleic acid (OA) treatment of HepG2 cells, TLR4, TNF $\alpha$ , and IL-6 levels were significantly decreased in the miR-182-5p group as compared with levels observed in controls. Following miR-182-5p administration, TLR4 mRNA and protein levels decreased along with those of TNF $\alpha$  and IL-6 proteins, and the liver weight/body weight ratio of treated mice was less than that observed in controls. Furthermore, hematoxylin and eosin staining showed that the miR-182-5p-treated group exhibited low adipose-cell cross-sectional areas, and Oil Red O staining showed decreases in the size of lipid droplets in the miR-182-5p-treated group. **Conclusions.** miR-182-5p ameliorated HFD-induced NASH by suppressing TLR4.

**Key words.** miR-182-5p. Non-alcoholic fatty liver disease. Non-alcoholic steatohepatitis. Toll-like receptor 4.

## INTRODUCTION

In recent years, the morbidity associated with nonalcoholic fatty liver disease (NAFLD), one of the most common liver diseases worldwide, in younger patients in many countries, such as China,<sup>1-3</sup> has increased. The most commonly accepted pathogenic mechanisms associated with nonalcoholic steatohepatitis (NASH) involve increased oxidative stress,<sup>4</sup> insulin resistance, and expression of inflammatory cytokines.<sup>5</sup>

The interest in Toll-like receptor (TLR) 4 in relation to NAFLD pathogenesis has increased.<sup>6-9</sup> Activation of TLR4 triggers intracellular signaling molecules, including myeloid differentiation factor (MyD88)-dependent and MyD88-independent pathways. MyD88-dependent path-

ways induce nuclear translocation of nuclear factor (NF)- $\kappa$ B, resulting in the production of inflammatory cytokines, such as interleukin (IL) 6 and tumor necrosis factor (TNF)  $\alpha$ , whereas MyD88-independent pathways promote the release of inflammatory cytokines, such as transforming growth factor  $\beta$ , IL6, and TNF $\alpha$ , which subsequently induce inflammation and the formation of fibrosis.<sup>10-12</sup> Moreover, the MyD88-dependent pathway was implicated in high-fat-diet (HFD)-induced NAFLD.<sup>8</sup>

MicroRNAs (miRNAs) are highly conserved, endogenous, noncoding RNA molecules that silence protein translation by binding to the 3' untranslated regions (3'UTRs) of target mRNA.<sup>13</sup> Analysis using TargetScan software ([http://www.targetscan.org/vert\\_71/](http://www.targetscan.org/vert_71/)) revealed that the sequence of miRNA-182-5p (miR-182-5p) de-

rived from a 4-kb region of murine chromosome 6q is complementary to the 3'UTR of mouse TLR4.

Currently, there are no reports regarding the role of miR-182-5p in HFD-induced nonalcoholic steatohepatitis in mice *in vivo*, as well as in lipopolysaccharide (LPS)-induced inflammatory response in RAW264.7 cells or oleic acid (OA)-induced lipid accumulation in HepG2 cells *in vitro*. Here, we studied the roles of miR-182-5p in the inflammatory response in macrophages following LPS administration, in lipid accumulation in HepG2 cells following OA administration, and in HFD-induced non-alcoholic steatohepatitis in mice to investigate miR-182-5p-related mechanisms associated with NAFLD.

## MATERIALS AND METHODS

### Cell cultures

The mouse macrophage cell line, RAW 264.7 (American Type Culture Collection, Rockville, MD, USA), was cultured in high-glucose DMEM (Invitrogen, CA, USA) supplemented with 10% fetal bovine serum (FBS; Invitrogen), and 1% (w/v) penicillin-streptomycin and streptomycin (100 µg/mL). Cells were fasted in serum-free medium for 12 h before stimulation with LPS. RAW264.7 cells were cultured in a six-well culture plate at a density of  $2-4 \times 10^5$  cells per well for 24 h, then the cells were transfected with 50 nM miR-182-5p mimic, miR-182-5p NC, and lip2000 (GenaPharma, Shanghai, China) for 24 h using Lipofectamine 2000 (Invitrogen) according to the manufacturer's instructions. Then, RAW264.7 cells were exposed to 1 µg/mL of LPS.

HepG2 cells were cultured in high-glucose DMEM supplemented with 10% fetal bovine serum and 1% (w/v) penicillin-streptomycin and streptomycin (100 µg/mL). Oleic acid (OA) was used as a steatosis vector of HepG2 cells. After reaching 30-40% confluence, the cultured cells in six-well plates were transfected with miR-182-5p mimic, miR-182-5p NC, and lip2000. Non-transfected HepG2 cells served as steatotic controls. After 24 h, the cells reached 80% confluence, and then the cells were exposed to 1.0 mmol/L OA, 1% FFA-free BSA, and 100 nmol/L long-acting insulin in DMEM.

All cells were incubated at 37°C in a humidified atmosphere with 5% CO<sub>2</sub>. Total RNA and total protein were extracted from harvested cells for mRNA and protein expression by RT-PCR and Western blotting, respectively.

### Animals

Twenty-four male C57BL / 6 mice were purchased from the Laboratory Animal Center of Nanjing Medical University at 3 weeks of age. All mice were kept in a spe-

cific pathogen-free facility under controlled light (06:00 am - 06:00 pm) and temperature ( $22 \pm 2^\circ\text{C}$ ) conditions with free access to tap water. After a 7-day adaptation period, the mice were randomly split into four groups of six mice each and fed a high-fat diet (HF; 4.73 kcal/g with 45% fat, 20% protein, and 35% carbohydrate; Mediceance Ltd., China) for a period of 12 weeks. Three groups of mice were administered 5 mg/kg of Ago- miR-182-5p (Ribobio, Guangzhou, China) via tail vein in saline (182-5p group), and miR-182-5p normal control (182-5p NC group) twice a week; the HF group was not treated. HFD and miR-182-5p NC groups were the control groups of HFD+miR-182-5p group. Body weight was monitored throughout life. After 12 weeks, the mice were killed at 09:00 am after overnight fasting (12 h). The animals in each cohort were sacrificed for liver and plasma collection. All animals were treated as recommended in the Guide for the Care and Use of Laboratory Animals, issued by the China Association of Laboratory Animal Care. All of the studies were approved by the University Committee on Use and Care of Animals and overseen by the Unit for Laboratory Animal Medicine at Nanjing Medical University.

### Real-time RT-PCR

Total RNA was isolated from tissue and cultured cells with TRIzol reagent (Invitrogen) and reverse-transcribed with a reaction mixture. Quantitative real-time PCR (qPCR) analysis was performed using the SYBR Green qPCR Master Mix (Applied Biosystems [ABI], CA, USA) and a Step One Plus real-time PCR system (ABI). The expression data were normalized to the expression of  $\beta$ -actin. To determine miRNA expression, total RNA was reverse-transcribed and the resulting cDNA was used with miRNA-specific TaqMan primers (ABI) and TaqMan Universal PCR Master Mix (ABI). RNU6B was used as an endogenous control for data normalization of miR-182-5p levels. The comparative threshold cycle (Ct) method was used to measure the relative changes in expression;  $2^{-\Delta\Delta\text{Ct}}$  represents the fold change in expression.

### Dual-luciferase reporter assays

For the 3'UTR luciferase reporter assay, the pmirGLO Dual-Luciferase miRNA Target Expression Vector (Promega, WI, USA) was used. The oligonucleotides were ligated into the NheI-XhoI site of pmirGLO. The RAW264.7 or HepG2 cells were co-transfected with the 182-5p mimic or its control, and constructed pmirGLO vectors and pRL-TK (Promega) using Lipofectamine 2000 for 24 h, according to the manufacturer's instructions. Firefly luciferase and Renilla luciferase luminescence was measured using the Dual-Glo luciferase Reporter Assay

System (Promega) and a GloMax 20/20 Luminometer (Promega). The ratios of Firefly luciferase luminescence relative to Renilla luciferase luminescence were calculated.

### Western analysis

Total protein from mouse livers or cells were obtained with lysis buffer (Beyotime, Nantong, China), resolved by SDS-polyacrylamide gel electrophoresis (PAGE), and transferred to an Immobilon-P polyvinylidene difluoride (PVDF; Millipore, MA, USA) membrane. After blocking the membranes using (5% wt/vol) skim milk for 60 min, the membranes were incubated with an anti-TLR4 antibody (Abcam, Cambs, UK), and anti- $\beta$ -actin antibody (Santa Cruz, CA, USA). After washing, the membranes were probed with the corresponding secondary antibodies before development using an ECL Western blotting detection system (Pierce, NJ, USA) by enhanced chemiluminescence.

### Immunoassay of Tumor Necrosis Factor- $\alpha$ and Interleukin-6

TNF- $\alpha$  and IL-6 levels were detected by ELISA according to the manufacturer's protocol (Adlitteram Diagnostic Laboratories anti-rat TNF- $\alpha$  Elisa kit and goat anti-rat IL-6 Elisa kit).

### Serum levels of triglycerides (TG)

A standard automatic analyzer (Hitachi 7600-10; Hitachi, Japan) was used to determine the serum levels of TG.

### The intraperitoneal glucose tolerance test (IPGTT)

Briefly, at W16, all the groups mice were fasted overnight. The mice injected i.p. with 1.5 g D-glucose (50% stock solution in saline)/kg body weight. Blood samples were taken from tail vein at 0-, 30-, 60-, and 120-min intervals after the glucose injection, and glucose levels were measured by a glucose meter (Accu-Chek; Roche).

### Histologic analysis

Formalin-fixed, paraffin-embedded mouse liver specimens were sectioned at 4 mm and stained with hematoxylin and eosin. Liver samples were also stained with picosirius red solution. The sections used for histopathologic analysis were examined by light microscopy. Liver samples were also stained with picosirius red solu-

tion, and the area of liver fibrotic was quantified using the winROOF visual system (Mitani Co., Tokyo, Japan).

### Assessment of lipid accumulation in HepG2 cells and liver tissues

Lipid accumulation in HepG2 cells was detected using Oil-red O staining. In brief, cells were washed with phosphate-buffered saline (PBS) and fixed with 4% (w/v) paraformaldehyde in PBS for 5 min. Then cells were incubated with 0.5% (w/v) Oil-red O in an isopropyl alcohol/water (60/40, v/v) solution for 30 min, and washed twice with PBS. The percentage of lipid-positive cells was analyzed with image software (Jeda, Jiangsu, China). Liver sections were stained with Oil-red O to detect TG. At least three slices per tissue sample ( $\times 100$  magnification) or three different microscopic fields per culture ( $\times 400$  magnification) were photographed. Each photograph was assessed by two investigators.

### NAFLD activity score (NAS)

The NAS, designed and validated by the Pathology Committee of the NASH Clinical Research Network, is used to assess the severity of NAFLD. An activity score was generated by adding the individual scores for the following features: steatosis ( $< 5\% = 0$ ;  $5 - 33\% = 1$ ;  $33 - 66\% = 2$ ;  $> 66\% = 3$ ); lobular inflammation (none = 0;  $< 2$  foci = 1;  $2 - 4$  foci = 2;  $> 4$  foci = 3); and ballooning (none = 0; few = 1; prominent = 2). A NAS  $< 3$  correlates with mild non-alcoholic fatty liver, a NAS of 3-4 correlates with moderate non-alcoholic fatty liver, and a NAS  $\geq 5$  correlates with NASH.

### Statistical analysis

Statistical analysis was performed using SPSS software (version 14.0; SPSS, Inc., Chicago, IL, USA). Significant differences between groups were analyzed by one-way ANOVA, followed by *post-hoc* Fisher's least significance difference (LSD) test. Body weight and serum glucose during IPGTT were analyzed by one-way ANOVA with repeated measures, followed by a LSD test. A  $P < 0.05$  was considered significant.

## RESULTS

### miR-182-5p reduces macrophage inflammatory response by inhibiting TLR4 expression

We used TargetScan version 5.2 to identify putative miR-182-5p-binding sequences in the 3'UTR of

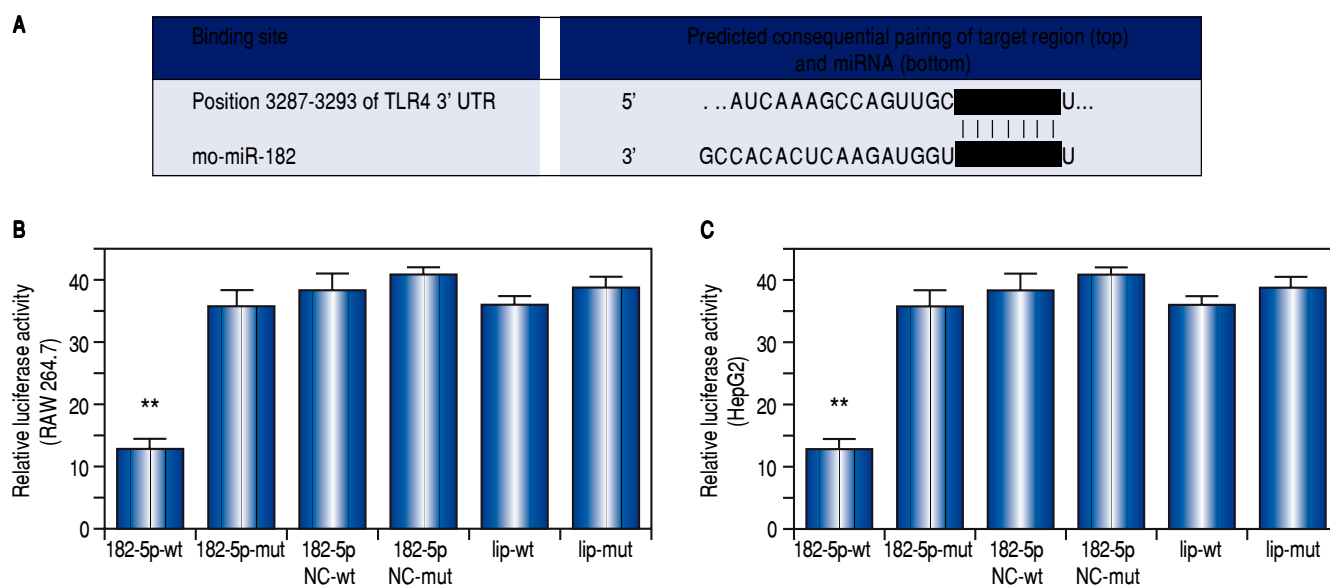


**Figure 1.** TLR4 is a miR-182-5p target according to dual-luciferase-reporter assay. **(A)** The putative miR-182-5p binding sequences in the TLR4 mRNA 3'-UTR according to TargetScan version 5.2. Transfection with a miR-182-5p mimic inhibits luciferase activity by more than 50% in **(B)** RAW264.7 and **(C)** HepG2 cells. \*\*  $P < 0.01$ , miR-182-5p group vs. other groups.

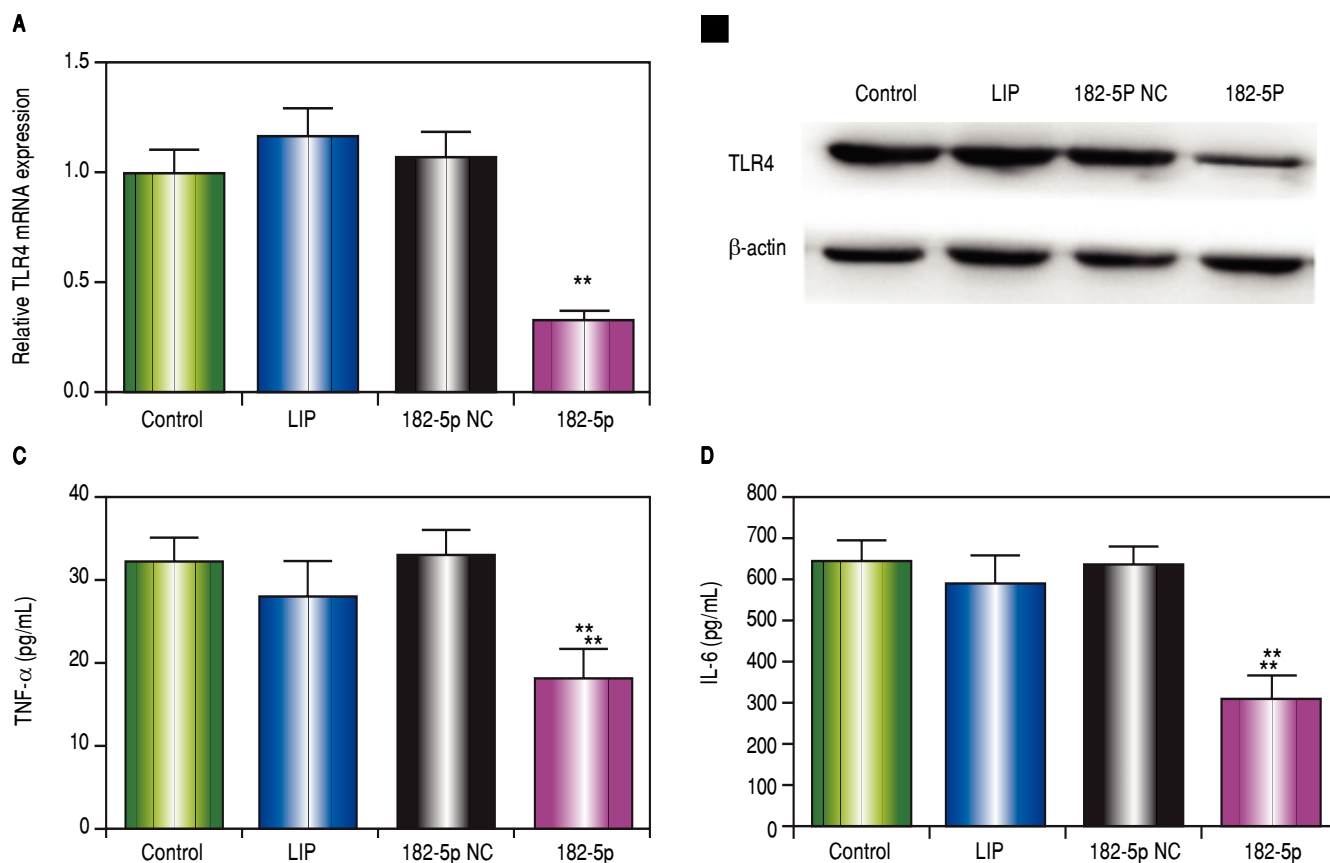


**Figure 2.** miR-182-5p down-regulates TLR4 in macrophages following LPS administration in vitro. **A.** RT-PCR analysis of TLR4 expression in macrophages following LPS administration. **B.** TLR4 protein levels according to western blot analysis. The levels of **(C)** TNF $\alpha$  and **(D)** IL-6 levels in supernatants according to ELISA. Results represent the mean  $\pm$  standard deviation. \* $P < 0.05$  and \*\* $P < 0.01$ , miR-182-5p group vs. other groups.

TLR4 (Figure 1A), and a luciferase reporter was used to confirm the role of miR-182-5p in TLR4 inactivation in macrophages. Our results verified that the miR-182-5p mimic inhibited luciferase activity by > 50% (Figure 1B), thereby demonstrating the ability of miR-182-5p to decrease TLR4 expression in macro-

phages. Additionally, transfection with the miR-182-5p mimic resulted in decreased TLR4 mRNA (Figure 2A) and protein (Figure 2B) levels in LPS-treated RAW264.7 cells. Furthermore, miR-182-5p transfection attenuated TNF $\alpha$  (Figure 2C) and IL-6 (Figure 2D) levels.

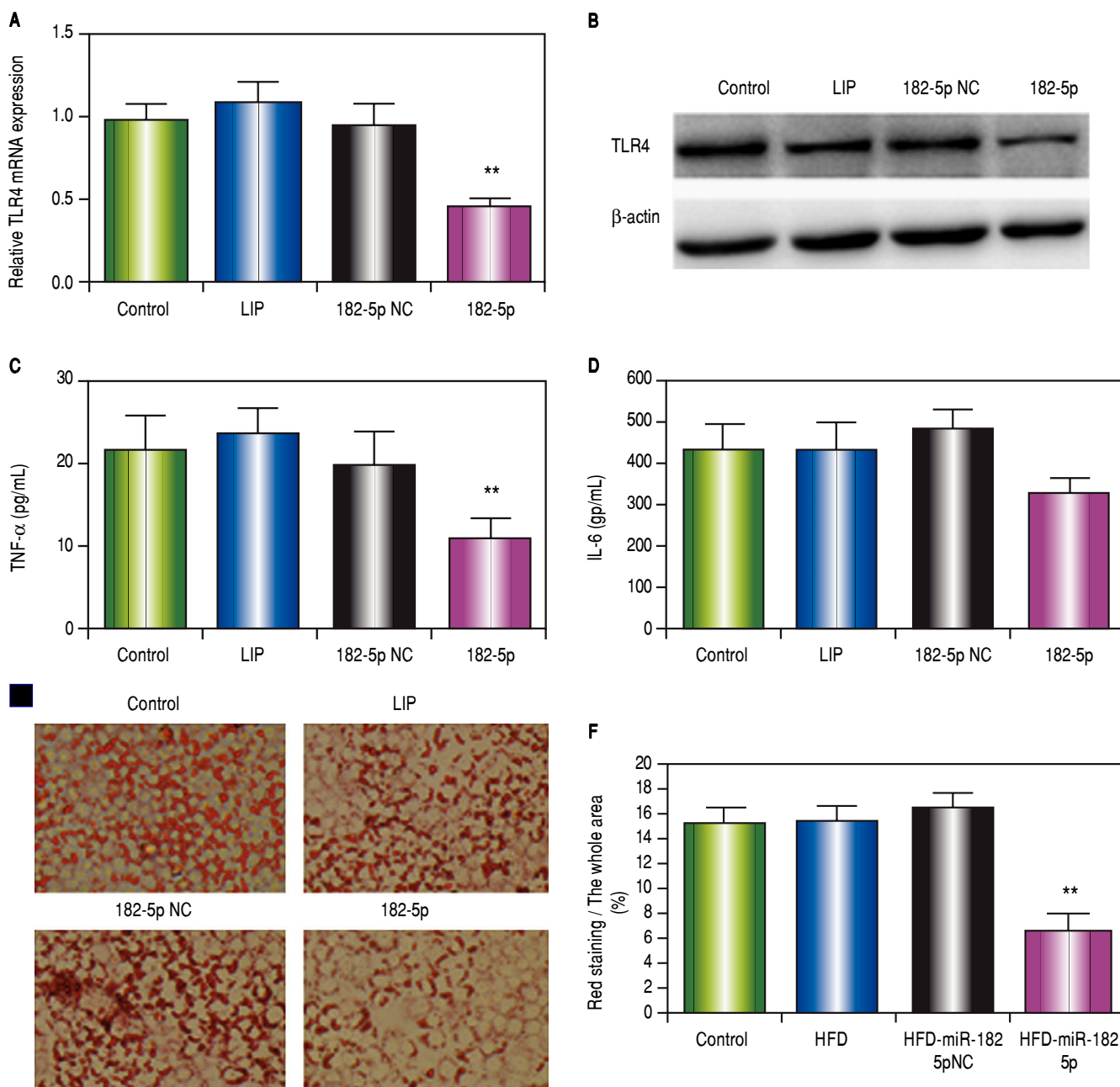


**Figure 3.** miR-182-5p down-regulates TLR4 in HepG2 cells following OA administration. **A.** RT-PCR analysis of TLR4 in HepG2 cells following OA administration. **B.** TLR4 protein levels according to western blot analysis. **C.** TNF $\alpha$  and **(D)** IL-6 levels in supernatants according to ELISA. **E** and **F.** Lipid accumulation decreased following miR-182-5p transfection. Results are the mean  $\pm$  standard deviation. \*  $P < 0.05$  and \*\*  $P < 0.01$ , miR-182-5p group vs. other groups.

### OA administration in miR-182-5p-transfected HepG2 cells downregulates TLR4 expression

OA-administered HepG2 cells transfected with the miR-182-5p mimic inhibited TLR4 mRNA (Figure 3A) and protein (Figure 3B) expression. miR-182-5p transfection also attenuated TNF $\alpha$  (Figure 3C) and IL-6 (Figure 3D) levels and decreased lipid accumulation (Figures 3E and 3F).

A luciferase reporter was used to confirm the role of miR-182-5p in TLR4 inactivation in HepG2 cells. Our results indicated that transfection with the miR-182-5p mimic inhibited luciferase activity by > 50% (Figure 1C), thereby demonstrating the ability of miR-182-5p to decrease TLR4 expression in hepatic parenchymal cells.

### Effects of miR-182-5p and HFD on the liver weight/body weight ratio and triglyceride (TG) levels in mice

As shown in figure 4G, the liver weight/body weight ratio in the HFD+miR-182-5p group was lower than that observed in HFD and HFD+miR-182-5p groups. The TG level in the HFD+miR-182-5p group was also lower than that observed in HFD and HFD+miR-182-5p groups (Figure 4H). The body weight in the HFD+miR-182-5p group was also lower than that observed in HFD and HFD+miR-182-5p groups at 16 weeks (Figure 5P).

### The intraperitoneal glucose tolerance test

The intraperitoneal glucose tolerance test show glucose levels in the HFD+miR-182-5p group was significantly reduced compared to the HFD, and HFD+miR-182-5p negative control (NC) groups at W16 (Figures 4E and 4F).

### Histologic changes

Hematoxylin and eosin staining in the control, HFD, HFD+miR-182-5p NC, and HFD+miR-182-5p groups revealed that the HFD+miR-182-5p group exhibited lower average adipose-cell cross-sectional areas as compared with the HFD and HFD+miR-182-5p NC groups (Figures 5E-5H).

### Assessment of lipid accumulation in liver tissue

As shown in figures 5B and 5C, Oil Red O staining indicated that the liver was filled with large droplets in the HFD and HFD+miR-182-5p NC groups; however, in the HFD+miR-182-5p group (Figure 5D), the lipid droplets were smaller. Oil-red O staining revealed lipid

droplets in 5.5% of cells in the HFD+miR-182-5p group; lipid droplets were found in 1.80%, 11.2%, and 10.6% of the cells in the NF, HFD, and HFD+miR-182-5p NC groups, respectively (Figure 5M).

### NAFLD Activity Score (NAS)

The severity of the NAFLD in the livers was assessed by NAS (Figure 5N). In HFD and HFD+miR-182-5p NC groups, NAS scores is 3.4 and 3.2, which show inflammation, liver steatosis, and ballooning was greater than the HFD+miR-182-5p group, which score is 1.2.

### Assessment of the fibrotic index in liver tissue

Picrosirius red solution was used to calculate the fibrotic index. The red-solution range for the miR-182-5p group (Figure 5L) was smaller than that observed for the HFD (Figure 5J) and HFD+miR-182-5p NC (Figure 5K) groups. The fibrotic index was significantly lower in HFD+miR-182-5p group than in HFD and HFD+miR-182-5p NC groups (Figure 5O).

## DISCUSSION

Our results indicated that the levels of TLR4 and pro-inflammatory cytokines decreased following miR-182-5p administration in a mouse model of HFD-induced NASH. Moreover, HFD-induced NASH attenuation was accompanied by decreases in TG levels and improved glucose tolerance.

Our previous studies demonstrated that the TLR4-signaling pathway is induced in a variety of liver pathological and physiological processes, including liver warm ischemia/reperfusion (I/R) injury,<sup>14</sup> graft injury in small-for-size liver transplantation,<sup>15,16</sup> and NASH pathogenesis,<sup>17</sup> which are all attenuated by inactivation of TLR4-signaling. In our previous study, we have shown miR-146b ameliorated HFD induced NASH by directly suppressing IL-1 receptor-associated kinase 1 (IRAK1) and tumor necrosis factor receptor-associated factor 6 (TRAF6), which are two key adaptor molecules downstream of TLR4. In this article, miR-182-5p directly inhibits the expression of TLR4, which also can ameliorate HFD-induced NASH. Therefore, miR-146b and miR-182-5p both can ameliorate HFD-induced NASH by inhibiting TLR4 signaling pathway.<sup>17</sup>

Moreover, we first verified that miR-182-5p can inhibit the expression of TLR4, and miR-182-5p can ameliorates liver I/R injury by targeting Toll-Like Receptor 4.18 Qin SB, *et al.* found that miR-182-5p inhibited apoptosis triggered and oxidative stress by targeting TLR4.<sup>19</sup>

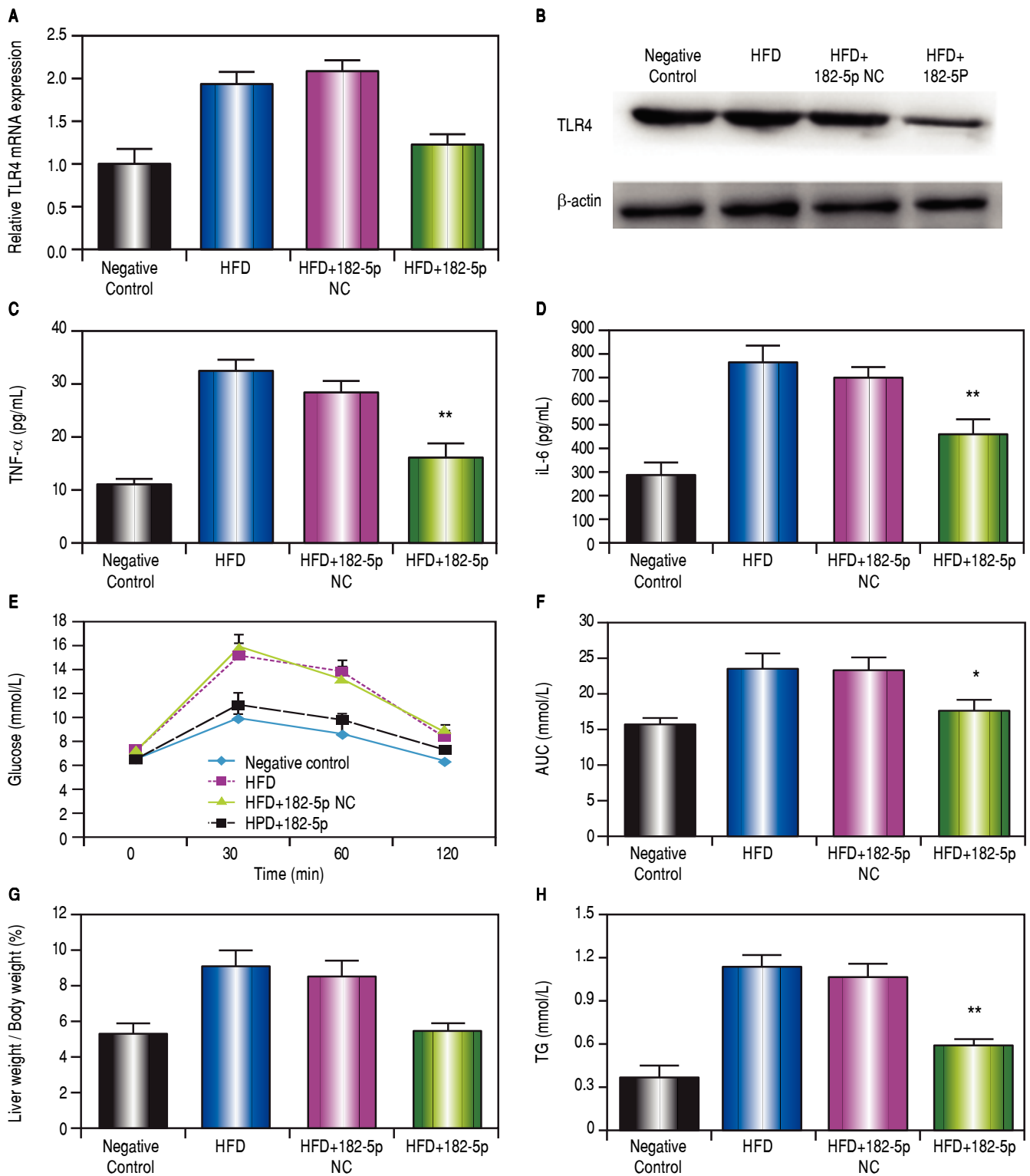


**Figure 4.** miR-182-5p downregulates TLR4 and decreases liver weight/body weight ratio and TG levels in HFD mice. (A) RT-PCR and (B) western blot analyses revealed significant decreases in TLR4 mRNA and protein levels, respectively, in the liver following miR-182-5p administration. (C) TNF $\alpha$  and (D) IL-6 levels in the liver decreased significantly following transfection with the miR-182-5p mimic. (E and F) Blood glucose area under the concentration-time curve (AUC) values for the 0-h to 2-h interval following glucose injection. (G) Liver weight/body weight ratio and (H) TG levels in the miR-182-5p group were lower than those observed in the HFD and HFD+miR-182-5p NC groups after 16 weeks. Results represent the mean  $\pm$  standard deviation. \*  $P < 0.05$  and \*\*  $P < 0.01$ , miR-182-5p group vs. HFD and HFD+miR-182-5p NC groups.

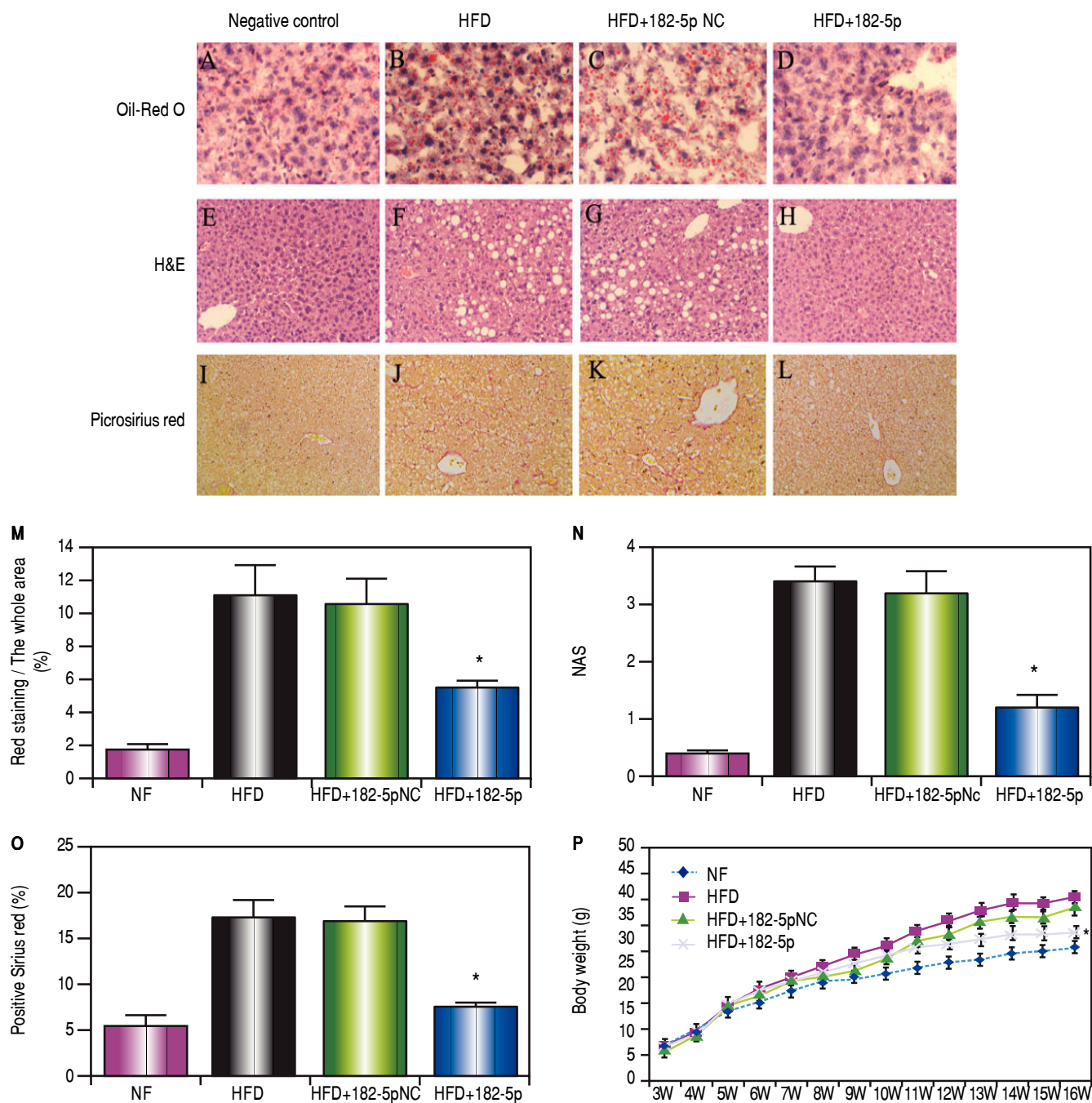


**Figure 5.** miR-182-5p decreased lipid accumulation in liver tissue and histological damage in HFD mice. **(A-D)** Representative Oil Red O staining in the NC, HFD, HFD+miR-182-5p NC, and HFD+miR-182-5p groups. **(B and C)** Livers of the HFD and HFD+miR-182-5p NC groups were filled with large droplets. **(D)** Livers of the miR-182-5p group were filled with small lipid droplets. **(E-H)** Representative hematoxylin and eosin staining in the NC, HFD, HFD+miR-182-5p NC, and HFD+miR-182-5p groups. **(F and G)** Livers of the HFD and HFD+miR-182-5p NC groups exhibited high average adipose-cell cross-sectional areas. **(H)** The miR-182-5p group exhibited low average adipose-cell cross-sectional areas as compared with areas observed in the **(F)** HFD and **(G)** HFD+miR-182-5p NC groups. **(I-L)** Representative picrosirius red staining to assess the fibrotic index in the NC, HFD, HFD+miR-182-5p NC, and HFD+miR-182-5p groups. The fibrotic index was significantly lower in the HFD+miR-182-5p group as compared with areas observed in the **(J)** HFD and **(K)** HFD+miR-182-5p NC groups. Data represent the mean  $\pm$  standard error of the mean ( $n = 6$ , each group). **(M)** Oil-red O staining revealed lipid droplets in 5.5% of cells in HFD+miR-182-5p group, which is lower than HFD and HFD+miR-182-5p NC groups. **(N)** The severity of the NAFLD in the mouse livers was assessed using the NAS. The NAS scores of HFD+miR-182-5p score is 0.7, which is lower than HFD and HFD+miR-182-5p NC groups. **(O)** The fibrotic index was significantly lower in HFD+miR-182-5p than HFD and HFD+miR-182-5p NC groups. **(P)** The body weight in the HFD+ miR-182-5p group was also lower than that observed in HFD and HFD+miR-182-5p groups at 16 weeks. \* $P < 0.05$ , miR-182-5p group vs. HFD and HFD+miR-182-5p NC groups.



TLR4 is potential therapeutic target for NASH.<sup>6-9,17</sup> Previous studies reported TLR4 effects on NASH pathogenesis in Kupffer cells;<sup>6,7</sup> however, Liang, et al.<sup>8</sup> showed that liver parenchymal cells also play a primary role in NASH pathogenesis. Moreover, we using TargetScan software found that the sequence of miR-182-5p is complementary to the 3'UTR of mouse TLR4. Based on these findings, we transfected different cells lines with an miR-182-5p mimic, with the results indicating significant suppression of TLR4 expression, as well as the downstream pro-inflammatory cytokines TNF $\alpha$  and IL-6, in both mouse macrophages and liver parenchymal cells. As a result, miR-182-5p can reduce the expression of inflammatory factors by inhibiting the expression of TLR4 *in vivo* and *in vitro*, and it can play a protective role for high-fat diet-induced nonalcoholic steatohepatitis in mice.

miR-182-5p also participates in developmental processes, including involvement in the regulation of circadian rhythms in the retina and cellular homeostasis in the inner ear.<sup>20,21</sup> In cancer processes, miR-182-5p is involved in apoptosis and cellular invasiveness.<sup>22-24</sup> In human gastric cancer cells, miR-182-5p improves the viability, migration, mitosis, and invasion ability by targeting the expression of RAB27A.<sup>25</sup> miR-182-5p can regulate the process of nerve injury-induced nociceptive hypersensitivity by inhibiting Ephrin Type-b Receptor 1.<sup>26</sup> These findings indicated that miR-182-5p may attenuate HFD-induced NASH through additional signaling pathways, which require further study.

In summary, our study revealed potential therapeutic roles for miR-182-5p based on its attenuation of NASH in a mouse model following miR-182-5p administration and overexpression. The underlying mechanism associated with this process might involve decreased inflammatory reactions in hepatic macrophages, as well as decreased inflammation and lipid metabolism in hepatic parenchymal cells.

## ABBREVIATIONS

- **ABI:** Applied Biosystems.
- **Ct:** threshold cycle.
- **HFD:** high-fat-diet.
- **I/R:** ischemia/reperfusion.
- **IL:** interleukin.
- **IRAK1:** IL-1 receptor-associated kinase 1.
- **LPS:** lipopolysaccharide.
- **LSD:** least significance difference.
- **miR-182-5p:** miRNA-182-5p.
- **miRNAs:** microRNAs.
- **NAFLD:** nonalcoholic fatty liver disease.
- **NAS:** NAFLD activity score.
- **NASH:** nonalcoholic steatohepatitis.
- **NC:** negative control.
- **NF:** nuclear factor.
- **OA:** oleic acid.
- **PBS:** phosphate-buffered saline.
- **PVDF:** polyvinylidene difluoride.
- **qPCR:** quantitative real-time PCR.
- **TG:** triglyceride.
- **TLR:** toll-like receptor.
- **TNF:** tumor necrosis factor.
- **TRAF6:** tumor necrosis factor receptor-associated factor 6.

## CONFLICT OF INTEREST

The authors declares that there is no conflict of interest regarding the publication of this article.

## SUPPORT

This study was supported by National Natural Science Foundation of China (81100318), Young medical talents in Jiangsu Province (QNRC2016081).

## ACKNOWLEDGMENTS

We thank Dr. Nan Zhou for the histologic analysis.

## REFERENCES

1. Rinella ME. Nonalcoholic fatty liver disease: a systematic review. *JAMA* 2015; 313: 2263-73.
2. Targher G, Chonchol MB, Byrne CD. CKD and nonalcoholic fatty liver disease. *Am J Kidney Dis* 2014; 64: 638-52.
3. Granér M, Nyman K, Siren R, Pentikäinen MO, Lundbom J, Hakkarainen A, Lauerma K, et al. Ectopic fat depots and left ventricular function in non-diabetic men with nonalcoholic fatty liver disease. *Circ Cardiovasc Imaging* 2015; 8: e001979.
4. Day CP, James OF. Steatohepatitis: a tale of two "hits"? *Gastroenterology* 1998; 114: 842-5.
5. Day CP. From fat to inflammation. *Gastroenterology* 2006; 130: 207-10.
6. Rivera CA, Adegboyega P, van Rooijen N, Tagalicud A, Allman M, Wallace M. Toll-like receptor-4 signaling and Kupffer cells play pivotal roles in the pathogenesis of non-alcoholic steatohepatitis. *J Hepatol* 2007; 47: 571-9.
7. Spruss A, Kanuri G, Wagnerberger S, Haub S, Bischoff SC, Bergheim I. Toll-Like Receptor 4 Is Involved in the Development of Fructose-Induced Hepatic Steatosis in Mice. *Hepatology* 2009; 50: 1094-104.
8. Li L, Chen L, Hu L, Liu Y, Sun HY, Tang J, Hou YJ, et al. Nuclear Factor High-Mobility Group Box1 Mediating the Activation of Toll-Like Receptor 4 Signaling in Hepatocytes in the Early Stage of Nonalcoholic Fatty Liver Disease in Mice. *Hepatology* 2011; 54: 1620-30.
9. Chen W, Wang X, Huang LI, Liu BO. Hepcidin in non-alcoholic fatty liver disease regulated by the TLR4/NF-kB signaling pathway. *Exp Ther Med* 2016; 11: 73-6.
10. Takeda K, Akira S. TLR signaling pathways. *Semin Immunol* 2004; 16: 329.

11. Seki E, Brenner DA. Toll-like receptors and adaptor molecules in liver disease: update. *Hepatology* 2008; 48: 322-35.
12. Akira S, Takeda K. Toll-like receptor signaling. *Nat Rev Immunol* 2004; 4: 499-511.
13. Ambros V. The functions of animal microRNAs. *Nature* 2004; 431: 350-5.
14. Jiang W, Kong L, Ni Q, Lu Y, Ding W, Liu G, Pu L, et al. miR-146a ameliorates liver ischemia/reperfusion injury by suppressing IRAK1 and TRAF6. *PLoS One* 2014; 9: e101530.
15. Jiang W, Ni Q, Tan L, Kong L, Lu Y, Xu X, Kong L. The microRNA-146a/b attenuates acute small-for-size liver graft injury in rats. *Liver Int* 2015; 35: 914-24.
16. Jiang W, Hu M, Rao J, Xu X, Wang X, Kong L. Over-expression of Toll-like receptors and their ligands in small-for-size graft. *Hepatol Res* 2010; 40: 318-29.
17. Jiang W, Liu J, Dai Y, Zhou N, Ji C, Li X. MiR-146b attenuates high-fat diet-induced non-alcoholic steatohepatitis in mice. *J Gastroenterol Hepatol* 2015; 30: 933-43.
18. Jiang W, Liu G, Tang W. MicroRNA-182-5p Ameliorates Liver Ischemia-Reperfusion Injury by Suppressing Toll-Like Receptor 4. *Transplant Proc* 2016; 48: 2809-14.
19. Qin SB, Peng DY, Shi Y, Ke ZP. MiR-182-5p Inhibited Oxidative Stress and Apoptosis Triggered by Oxidized Low-Density Lipoprotein via Targeting Toll-Like Receptor 4. *J Cell Physiol* 2017 [Epub ahead of print].
20. Xu S, Witmer PD, Lumayag S, Kovacs B, Valle D. MicroRNA (miRNA) transcriptome of mouse retina and identification of a sensory organ-specific miRNA cluster. *J Biol Chem* 2007; 282: 25053-66.
21. Li H, Kloosterman W, Fekete DM. MicroRNA-183 family members regulate sensorineural fates in the inner ear. *J Neurosci* 2010; 30: 3254-63.
22. Guttilla IK, White BA. Coordinate regulation of FOXO1 by miR-27a, miR-96, and miR-182 in breast cancer cells. *J Biol Chem* 2009; 284: 23204-16.
23. Chiang CH, Hou MF, Hung WC. Up-regulation of miR-182 by  $\beta$ -catenin in breast cancer increases tumorigenicity and invasiveness by targeting the matrix metalloproteinase inhibitor RECK. *Biochim Biophys Acta* 2013; 1830: 3067-76.
24. Rasheed SA, Teo CR, Beillard EJ, Voorhoeve PM, Casey PJ. MicroRNA-182 and microRNA-200a control G-protein subunit alpha-13 (GNA13) expression and cell invasion synergistically in prostate cancer cells. *J Biol Chem* 2013; 288: 7986-95.
25. Li Y, Chen S, Shan Z, Bi L, Yu S, Li Y, Xu S. miR-182-5p improves the viability, mitosis, migration, and invasion ability of human gastric cancer cells by down-regulating RAB27A. *Biosci Rep* 2017; 37: pii: BSR20170136.
26. Zhou X, Zhang C, Zhang C, Peng Y, Wang Y, Xu H. MicroRNA-182-5p Regulates Nerve Injury-induced Nociceptive Hypersensitivity by Targeting Ephrin Type-b Receptor 1. *Anesthesiology* 2017; 126: 967-77.

**Correspondence and reprint request:**

Weiwei Jiang, M.D.

Department of Neonatal Surgery, Children's Hospital of Nanjing Medical University,  
72 Guangzhou Road, Nanjing 210008, China.  
E-mail: wwjiang@njmu.edu.cn